Climatic Change (2016) 139:265–278
DOI 10.1007/s10584-016-1781-3

Enhancement of heavy daily snowfall in central Japan due to global warming as projected by large ensemble of regional climate simulations

Hiroaki Kawase[1] · **Akihiko Murata**[1] · **Ryo Mizuta**[1] · **Hidetaka Sasaki**[1] · **Masaya Nosaka**[1] · **Masayoshi Ishii**[1] · **Izuru Takayabu**[1]

Received: 13 January 2016 / Accepted: 17 August 2016 / Published online: 31 August 2016

Abstract This study investigates future changes in the accumulated and daily heavy winter snowfall in central Japan and the surrounding regions. We analyze outputs of the 48-member ensemble regional climate simulations in the historical and future climates. In the historical climate simulations, each ensemble member has a 61-year simulation from September 1950 to August 2011. For the future climate simulations, we also conduct 61-year simulations assuming the climate at the end of the twenty-first century (2080–2099) when the global mean surface air temperature is about 4 °C warmer than the pre-industrial climate (1861–1880) as projected under the Representative Concentration Pathway (RCP) 8.5 scenario. Our simulations show that the heavy snowfall occurring at a frequency of every 10 years is enhanced in the inland areas of the central part of the Japanese archipelago (central Japan) where the total winter snowfall amount decreases significantly. Heavy snowfall is also intensified in the northern part of the Asian continent where the surface air temperature is much colder than over central Japan. A composite analysis of heavy snowfall events in central Japan indicates that such events occur when the Japan Sea polar air mass convergence zone (JPCZ) appears during the East Asian winter monsoon season. In the future climate projections, the JPCZ is intensified since the warm ocean supplies more moisture due to warming. An upward wind anomaly is also found over the windward side of mountains where the upward flow is prevalent climatologically. The intensification of both the JPCZ and the upward wind over the mountain ranges result in the enhancement of heavy snowfall in inland areas where the surface air temperature is still below 0 °C.

Electronic supplementary material The online version of this article (doi:10.1007/s10584-016-1781-3) contains supplementary material, which is available to authorized users.

✉ Hiroaki Kawase
hkawase@mri-jma.go.jp

[1] Meteorological Research Institute, Japan Meteorological Agency, 1-1, Nagamine, Tsukuba, Ibaraki 305-0052, Japan

1 Introduction

Observations have indicated a decrease in extent of snow cover in the Northern Hemisphere in the recent decades (Vaughan et al. 2013). The melting of snow and ice due to global warming reduces the albedo, which accelerates global warming through an ice-albedo feedback (Armstrong and Brun 2008). On the other hand, the snow water equivalent (SWE) is projected to increase at the end of the twenty-first century over regions where the winter surface air temperature is extremely low in the present climate based on the Coupled Model Intercomparison Project Phase 3 (CMIP3) multimodel dataset (Brown and Mote 2009).

Since snowfall and snow cover are strongly influenced by the complicated shapes of mountains, high-resolution regional climate simulations, i.e., dynamical downscaling using regional climate models, have been conducted in individual regions to examine the changes in the future climate (e.g., Rasmussen et al. 2011; Steger et al. 2012; Kawase et al. 2013). In the Colorado headwater region, climate change due to global warming enhances the conversion of snowfall to rainfall and the melting of the snowpack at its lateral boundary, while snowfall increases at the center of the snowpack (Rasmussen et al. 2011). The declines in snowfall are notable at higher altitudes or higher latitudes, wherein the areas of strong reductions roughly coincide with the shift in the 0 °C line (Wi et al. 2012). Räisänen and Eklund (2012) pointed out the future decrease in SWE in northern Europe, although winter precipitation increases. They also found a slight increase in the mean SWE locally in the mountains of northern Sweden in March.

East Asian countries are also concerned about future changes in snowfall and snow cover. In the central parts of the Japanese archipelago (hereafter referred to as central Japan), more than 5 m of snow depth is observed over the mountainous area, which is one of the heaviest snowfall areas in the world (Kawase et al. 2015a). It is anticipated that global warming would cause dramatic changes in Japan's winter condition. Snowfall and snow depth are sensitive to climate changes since the winter mean temperature in the Japanese archipelago, which is around 0 °C except for high mountains, is higher than in other mid-latitude regions due to the surrounding oceans. Plentiful snow in the mountains is important for water resources in spring and summer agriculture, and the generation of hydraulic power in Japan. Hence, future changes in snow and its seasonal march will dramatically affect water resources, such as river discharge (Ma et al. 2010).

In China and the Korean Peninsula, heavy snowfall is brought by migratory extratropical cyclones and the expansion of the Siberian High in the Korean Peninsula and China (Heo and Ha 2008; Lim and Hong 2007; Sun et al. 2010). Sun et al. (2010) projected that global warming would cause a decrease in the frequency of intense snowfalls over southern China, while it would initially increase and then decrease in the twenty-first century over northern China.

Collins et al. (2013) indicated that the frequency and intensity of heavy precipitation would increase over land due to global warming. As with heavy rainfall, there are risks brought by heavy snowfall, such as surface avalanches in mountainous areas, traffic hindrances, and the isolation of villages through road closures. If the total amount of snowfall decreases and extremely heavy snowfall is unchanged or increases due to global warming, adaptation to global warming would be harder due to the snowfall changes. Some studies have investigated future changes in extremely heavy snowfall events (e.g., O'Gorman 2014; de Vries et al. 2014; Lute et al. 2015). Large reductions in extreme snowfalls are projected in Europe and the U.S. due to global warming, except for the coldest areas such as the Alps and the Rocky Mountains

(de Vries et al. 2014; Lute et al. 2015). In this study, we evaluate future changes in extremely heavy daily snowfall events in Japan based on 48-member ensemble regional climate simulations. We also analyze snowfall changes in the surrounding regions, such as the eastern parts of the Asian continent, and compare them with snowfall changes in Japan.

2 Model description and simulation design

We used the database for Policy Decision making for Future climate change (d4PDF) that contains a large number of historical and future ensemble climate simulations with high-resolution atmospheric models. An outline of the d4PDF is provided below, and detailed descriptions are given in Supplementary Texts S1 and S2. The simulation design of the ensemble experiments is also summarized in Table S4.

Global climate simulations were conducted using Meteorological Research Institute atmospheric general circulation model 3.2 (MRI-AGCM3.2) (Mizuta et al. 2012) with 60-km horizontal grid spacing. Historical climate simulations were conducted from 1950 to 2011 using the historical sea surface temperature (SST) database of COBE-SST2 (Hirahara et al. 2014). We conducted 100-member ensemble simulations with perturbed atmospheric initial and lower boundary conditions. The spread of SST perturbations is mostly equivalent to the analysis error of COBE-SST2. Perturbations of sea ice concentrations and thickness were given to the model, which is consistent with the SST. Future climate projections were performed with SSTs under global warming conditions when the global mean surface air temperature is 4 °C higher than the pre-industrial condition (1861–1880). Future SST distributions are provided by six coupled general circulation models (CGCMs) participating in Coupled Model Intercomparison Project Phase 5 (CMIP5). The CGCMs were selected using a cluster analysis of the horizontal patterns of SST changes (ΔSSTs) between 1991 and 2010 in the historical simulations and 2080–2099 under the Representative Concentration Pathway 8.5 (RCP 8.5) scenario (Mizuta et al. 2014). Since each CGCM shows a different range of warming at the end of the twenty-first century, the ΔSSTs of each CGCM are scaled by multiplying a single factor (Supplementary Table S1 and Text S2) so that the atmospheric general circulation model (AGCM) simulation forced by future SSTs shows a 4 °C warming in the global mean surface air temperature. We conducted 90-member ensemble simulations using 15 sets of the perturbed initial and boundary conditions for each of the 6 ΔSSTs. The future climate simulations were conducted for 62 years, which is the same as the historical simulations. Note that only the simulations from 1951 to 2010 (60 years) are officially provided in d4PDF.

Based on the global historical and future climate simulations, regional climate simulations were conducted using the non-hydrostatic regional climate model (NHRCM; Sasaki et al. 2008) with 20-km horizontal grid spacing. See Supplementary Table S3 for detailed specifications of the NHRCM. The NHRCM covers all of the islands of Japan, the Sea of Japan, and the eastern parts of the Asian continent. Regional climate simulations of historical climate have 50 ensemble members due to limited computational resources for making the d4PDF dataset. The historical climate simulations are conducted from 20 July 1950 to 31 August 2011 based on the historical global climate simulations. We also conducted 90 ensemble members of 61-year simulations based on the global climate simulations for climate at the end of the twenty-first century. In order to have same number of ensemble members in the historical and future simulations in this study, we analyzed 48 ensemble members of each type of simulation. Since

the maximum ensemble size of the historical simulations is 50. The reason for 48 members is that samples of each ΔSST can be considered equally, i.e., six ΔSSTs with eight sets of perturbations.

The available samples comprise 2928 years of both historical and future simulations (see Table S4). This paper focuses on the winter season, which is defined as the 5 months from November to March.

The skill of the NHRCM was evaluated by the Automated Meteorological Data Acquisition System (AMeDAS), administered by the Japan Meteorological Agency. AMeDAS is a dense network of meteorological stations throughout Japan; an average interval is approximately 17 km. Winter precipitation is overestimated by approximately 30 %. The overestimation of winter precipitation is remarkable inland and on the Pacific Ocean coast (Supplementary Fig. S2a), which has been pointed out by Ishizaki et al. (2012) and Kawase et al. (2015b). Note that most AMeDAS stations attached wind guards after the late 1990s. The details of model evaluation are discussed in Supplementary Text S3.

3 Future changes in daily snowfall extremes

Future climate simulations show the southern and southeastern anomalies prevailing over the Sea of Japan and the Pacific Ocean (Supplementary Fig. S3), which means the northwesterly winds, i.e., the East Asian Winter Monsoon (EAWM), will weaken. The dry northwesterly winds from the continent obtains abundant moisture from the Sea of Japan and uplifts the Japanese mountains, causing much precipitation along the Sea of Japan coast (Manabe 1957). Therefore, the weakening of the northwesterly winds results in a decrease in winter precipitation on the Sea of Japan coast (Supplementary Fig. S3). Here, winter refers to the 5 months from November through March (NDJFM). On the other hand, the total winter snowfall amount (hereafter referred to as SNF_TOTAL) largely decreases in most parts of Japan (Fig. 1a). The SNF_TOTAL increases only in the central part of northern Japan and the northern part of the Asian continent where the winter mean temperature is much lower than the freezing point of water. In the meantime, heavy daily snowfall amounts occurring approximately once every 10 years (hereafter referred to as SNF_10Y) are intensified in the inland areas of Central Japan, the northern part of Japan, and the northern part of the Asian continent (Fig. 1b).

Figure 1c shows the topography of central Japan and the locations of typical coastal and inland mountainous grid points (hereafter referred to as GP_COAST and GP_INLAND), which correspond to Niigata City and Tsunan Town, respectively. Figure 2a and b show the frequencies of the daily snowfall intensities at GP_COAST and GP_INLAND. Here, days of no snowfall (precipitation) are defined as days when snowfall (precipitation) is less than 0.1 mm. The snowfall in AMeDAS is estimated from the precipitation when the surface air temperature is lower than 0.5 °C. The frequency of weak daily snowfall is well simulated by the NHRCM at GP_COAST except for the 0–2 mm range, while the simulated heavy daily snowfall is less frequent than the observation. In GP_INLAND, the frequency of heavy daily snowfall is overestimated, which may result from the elevation difference between the actual topography (452 m) and the NHRCM topography (approximately 732 m).

The number of days with snowfall obviously decreases in most snowfall intensity bins at GP_COAST in future climate simulations, while the number of days without snowfall increases (Fig. 2a). In contrast, the frequency of heavy snowfall events of more than 50 mm/day increases at GP_INLAND (Fig. 2b). Figure 2c and d illustrate the cumulative

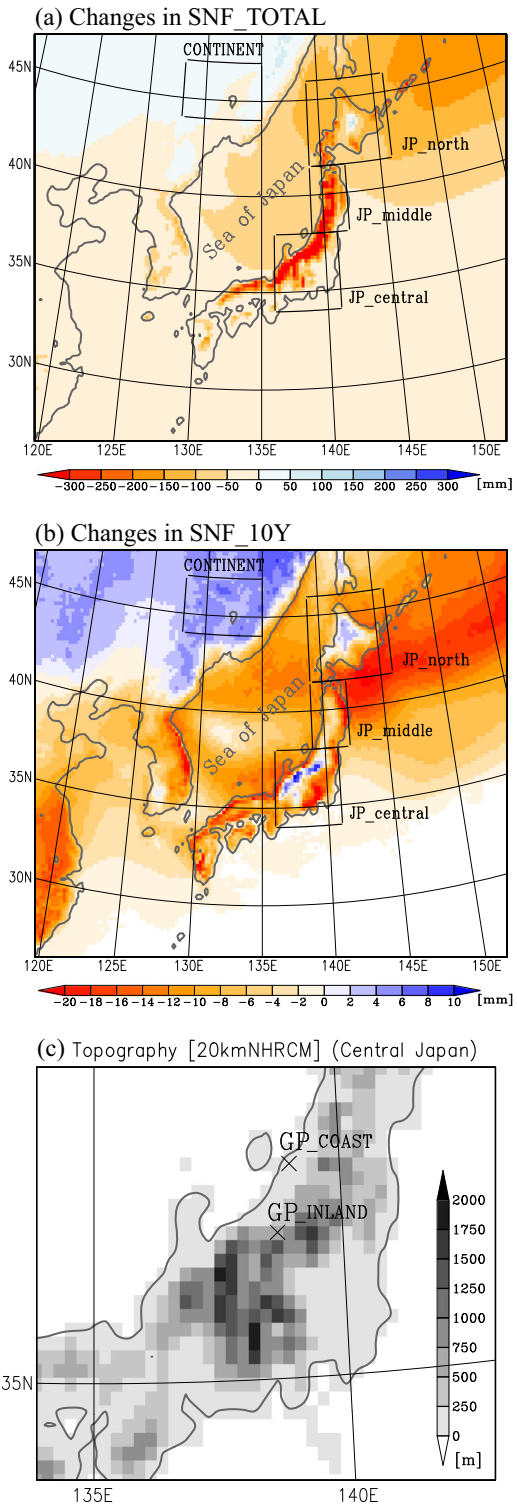

Fig. 1 Changes in (**a**) the winter total snowfall (SNF_TOTAL) and (**b**) heavy snowfall once every 10 years (SNF_10Y); (**c**) topography in Central Japan and the locations of GP_COAST and GP_INLAND

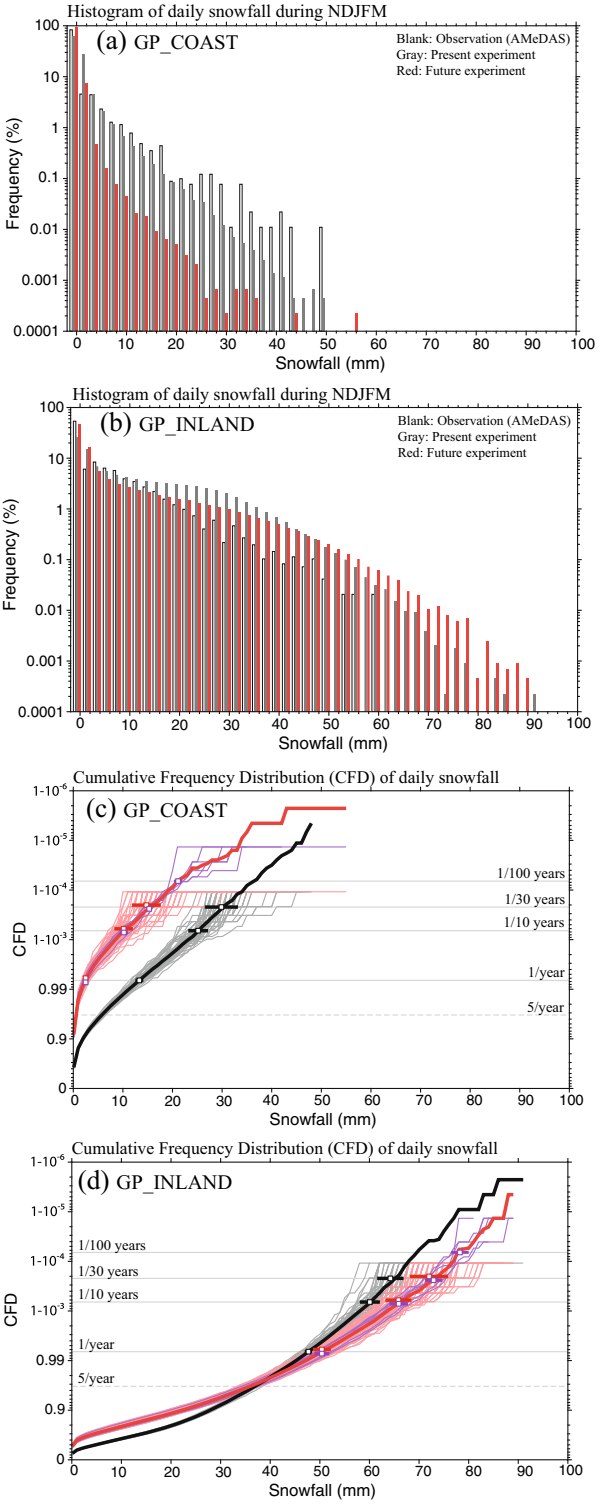

Fig. 2 Frequency of each daily snowfall intensity (%) at (**a**) GP_COAST and (**b**) GP_INLAND, and the cumulative frequency distribution (CFD) of daily snowfall at (**c**) GP_COAST and (**d**) GP_INLAND calculated in historical (*gray*) and future (*red*) simulations. *Blank bars* represent snowfall in AMeDAS stations, which is estimated by the precipitation and air temperature (less than 0.5 °C). The y-axes are logarithmic axes. In (**c**) and (**d**), *thick black* and *red lines* represent 48 ensemble members of the historical and future climate simulations, respectively. *Thin gray* and *red lines* represent ensemble members in the historical and future climate simulations, respectively. *Thin purple lines* represent the six future climate simulations as classified by ΔSST. *Squares* and *thick horizontal bars* represent the averages and ranges of one standard deviation, respectively, estimated by all ensemble members in the historical (*black*) and future (*red*) climate simulations, and six ΔSST ensemble members in the future climate simulations (*purple*)

frequency distributions of daily snowfall at GP_COAST and GP_INLAND, respectively. Figure 2 includes all daily snowfall in winter, not the maximum daily snowfall in each year. The probability of heavy daily snowfall occurring once every year corresponds to 1/151.25 = $6.61 * 10^{-3}$ where 151.25 is the average of days from November to April. Heavy snowfall events, with an occurrence frequency of less than five times a year, increase at GP_INLAND in the future climate. The SNF_10Y in the future climate is approximately 10 % larger than that in the historical climate simulation at GP_INLAND, which is a significant change at the 95 % confidence level, according to the Student t-test, as estimated by the ensemble members (Fig. 2d). In other words, heavy daily snowfall occurs more frequently in the future climate than in the historical climate simulations. Future precipitation, including snowfall and rainfall, increases in most ranges of precipitation intensity, while the number of precipitation days decreases at both GP_COAST and GP_INLAND (Figure not shown).

The future changes in the SNF_TOTAL and SNF_10Y would depend on the winter mean surface air temperature in the historical simulations (hereafter referred to as *TAS_ winter*). A map of TAS_winter is shown in Supplemental Figure S4. In addition, the relationship between TAS_winter and the future changes in SNF_10Y depends on the regions according to Fig. 1b. Here, we focus on the four regions shown in Fig. 1: CONTINENT, JP_north, JP_middle, and JP_central. Figure 3a shows the relationship between TAS_winter and the future changes in the SNF_TOTAL at each grid point of the four regions. The TAS_winter and SNF_TOTAL changes show a clear negative correlation. A correlation coefficient of the TAS_winter and SNF_TOTAL is −0.92. The regressions are similar in the regions, except for JP_north (Fig. 3a and Supplementary Table S5). The SNF_TOTAL dramatically decreases in warm areas, e.g., more than a 50 % decrease relative to the historical climate simulation in areas where the TAS_winter exceeds 5 °C. In cold areas, such as JP_north and CONTINENT, there appears to be a relatively small reduction in SNF_TOTAL where TAS_winter ranges roughly from −5 °C to 0 °C in the historical climate simulations. Moreover, SNF_TOTAL increases, probably due to increased atmospheric water vapor over the extremely cold areas where TAS_winter is lower than −5 °C in the historical climate simulations.

The relationship between the future changes in TAS_winter and SNF_10Y also shows a negative correlation (Fig. 3b), while the decreasing rate of SNF_10Y to TAS_winter is smaller than that of SNF_TOTAL. All grid points in Fig. 3b are more scattered than those in Fig. 3a. The correlation coefficients of the SNF_10Y and TAS_winter are smaller than those of the SNF_TOTAL and TAS_winter. In Fig. 3b, the distribution in each region is more scattered than that in Fig. 3a, except for CONTINENT. Individual regions have their own regressions. In JP_central, it is noteworthy that the SNF_10Y in the future climate is about 10 % larger than SNF_10Y in the historical climate simulations, although the TAS_winter is in a range from 0 °C to 5 °C. No future intensification in SNF_10Y is simulated in JP_middle. In most of CONTINENT and part of JP_north where TAS_winter is lower than 0 °C, SNF_10Y is projected to be intensified in the future climate.

Figure 3c shows the relationship between future changes in SNF_TOTAL and SNF_10Y. It is apparent that the future SNF_10Y decreases at a smaller rate than that of SNF_TOTAL. In most parts of Japan, both SNF_TOTAL and SNF_10Y decrease. On the other hand, over JP_central and JP_north, SNF_10Y is intensified at some grid points, although SNF_TOTAL decreases almost everywhere. In most parts of CONTINENT and several parts of JP_north, both SNF_TOTAL and SNF_10Y increase in the future.

We investigated the frequency of heavy daily snowfalls with more than 65 mm/day, which is approximately the 100th heaviest snowfall event at GP_INLAND in the historical

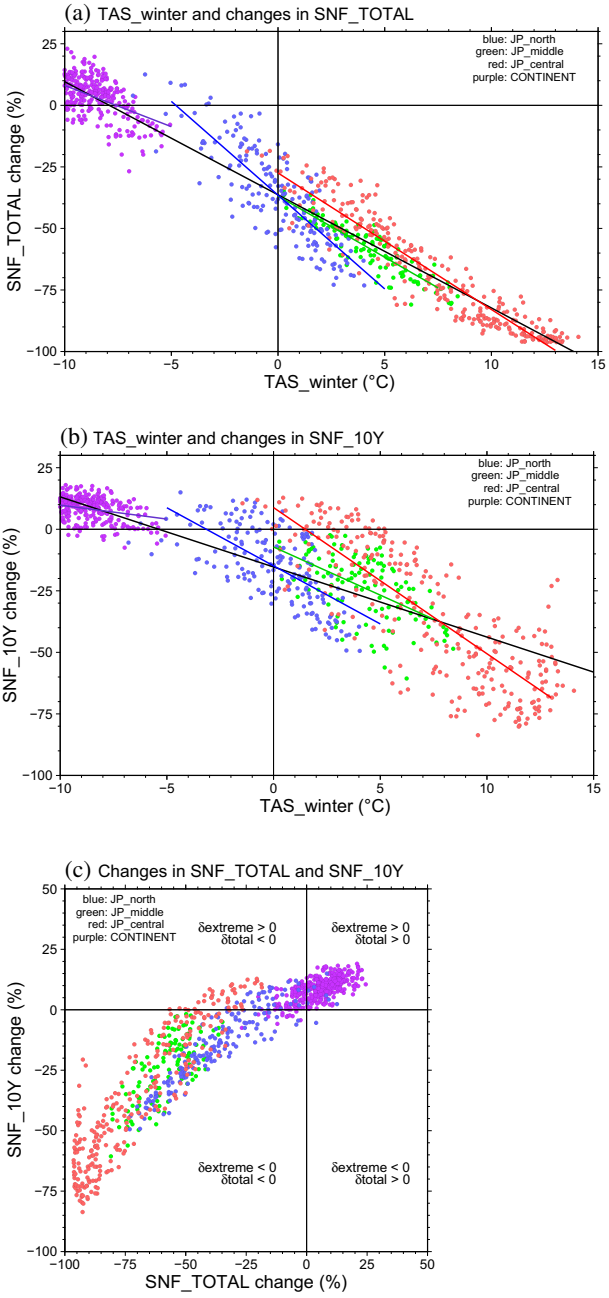

Fig. 3 Relationships between (**a**) changes in the SNF_TOTAL and surface air temperature from November to March (TAS_winter) in the historical climate simulations, (**b**) changes in the SNF_10Y and TAS_winter, and (**c**) changes in the SNF_10Y and SNF_TOTAL. *Blue*, *green*, *red*, and *purple circles* represent land grid points in JP_north, JP_middle, JP_central, and CONTINENT, respectively, in Fig. 1. *Solid lines* show the regressions in the individual regions (*colored lines*) and all 4 regions (*black line*)

simulations. The total number of events is 105 in the historical simulations and 352 in the future climate simulations. In the historical climate simulations, 52 events occur in December, which is about half of the total. The other events mainly occur in November (22 events) and January (22 events). In the future simulations, the frequency decreases remarkably in November (9 events). In contrast, the frequency becomes three and six times higher than in

the historical climate simulations in December (177 events) and January (132 events), respectively. In addition, 30 events occur in February in the future climate simulations, which is approximately seven times more frequent than in the historical climate simulations (4 events). In March, few events occur in either the historical (5 events) or the future (4 events) climate simulations.

4 Synoptic conditions of extremely heavy snowfall in central Japan

As discussed in Section 3, the inland area of central Japan is a peculiar region where the total snowfall would decrease but heavy daily snowfall could increase under global warming conditions. We analyzed the synoptic conditions when extremely heavy snowfall occurs in central Japan. A composite analysis of extremely heavy snowfall events in central Japan indicates that extremely heavy precipitation occurs when northwesterly winds, i.e., the EAWM, prevails and a convergence zone, called the Japan Sea polar air mass convergence zone (JPCZ) (Nagata et al. 1986), is generated over the Sea of Japan (Fig. 4a). Here, we picked the top 50 heavy snowfall events of GP_INLAND across all ensemble members in both historical and future climate simulations. In the future climate simulations, it is evident that precipitation increases around the JPCZ and on the Sea of Japan coast in central Japan. Surface wind anomalies suggest the intensification of the JPCZ (Fig. 4b).

Figure 5a illustrates the vertical cross section of the vertical wind speed across the JPCZ (See SW-NE in Fig. 4). The strong upward flow in the middle of Fig. 5a corresponds to the JPCZ. It is clear that the upward flow of the JPCZ strengthens during extremely heavy snowfall events in the future climate simulations. The downward flow also intensifies around the JPCZ on the northeastern side, which is related to the reduction in precipitation (Fig. 4b). Atmospheric warming is larger at the lower layers (Supplementary Fig. S5), meaning that vertical atmospheric stability would be more unstable. On the other hand, the latent heat flux increases over the Sea of Japan (Supplementary Fig. 6), meaning that the warmer ocean supplies more water vapor to the atmosphere in the future climate. Figure 5b shows that more water vapor is concentrated around the JPCZ, compared with the historical climate simulations. Since condensation releases latent heat, the high concentration of water vapor around the convergence zone contributes to the stronger development of the cumulus convection in the future climate. On the other hand, Fig. 4b shows slightly intensified northwesterly winds, which could also contribute to the intensification of the JPCZ.

Figure 5c shows a vertical cross section across the mountainous area (NW-SE in Fig. 4) that is perpendicular to the climatological northwesterly winds. The upward flow anomaly is found over the windward side of mountains where the upward wind is prevalent climatologically due to the EAWM. The stronger northwesterly flow in the warmer climate could interact with the inland mountains, contributing to the enhancement of the windward precipitation. The horizontal wind anomaly is, however, small in the northwestern side of the mountains that is the windward side under the EAWM (Figs. 4b and 5c). Moistening (Fig. 5d) and less stable atmosphere (Supplementary Fig. S5) would enhance the upward flow, as with the JPCZ. It has been pointed out that upward and downward winds could be strengthened over the windward and leeward of mountain ranges, respectively, due to global warming, and precipitation could be enhanced around the mountains (e.g., Shi and Durran 2015; Siler and Roe 2014). The enhancement of both the JPCZ and the upward wind over the mountain ranges could result in heavy snowfall in the mountains.

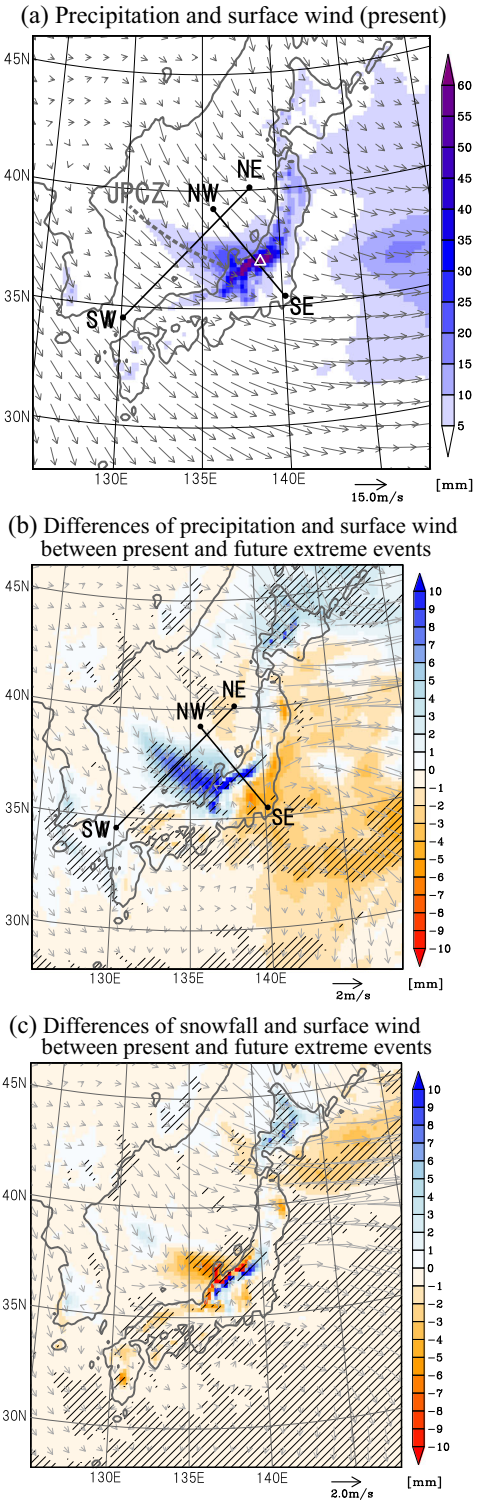

Fig. 4 **a** Composite of the surface wind and precipitation of the top 50 daily snowfall events at GP_INLAND in the historical simulations, and differences between historical and future simulations in (**b**) the surface winds and precipitation, and (**c**) the surface winds and snowfall of the top 50 daily snowfall events in the historical and future simulations. The triangle marks the location of GP_INLAND. *Hatched areas* represent significant changes at the 95 % confidence interval, according to the Mann-Whitney U test

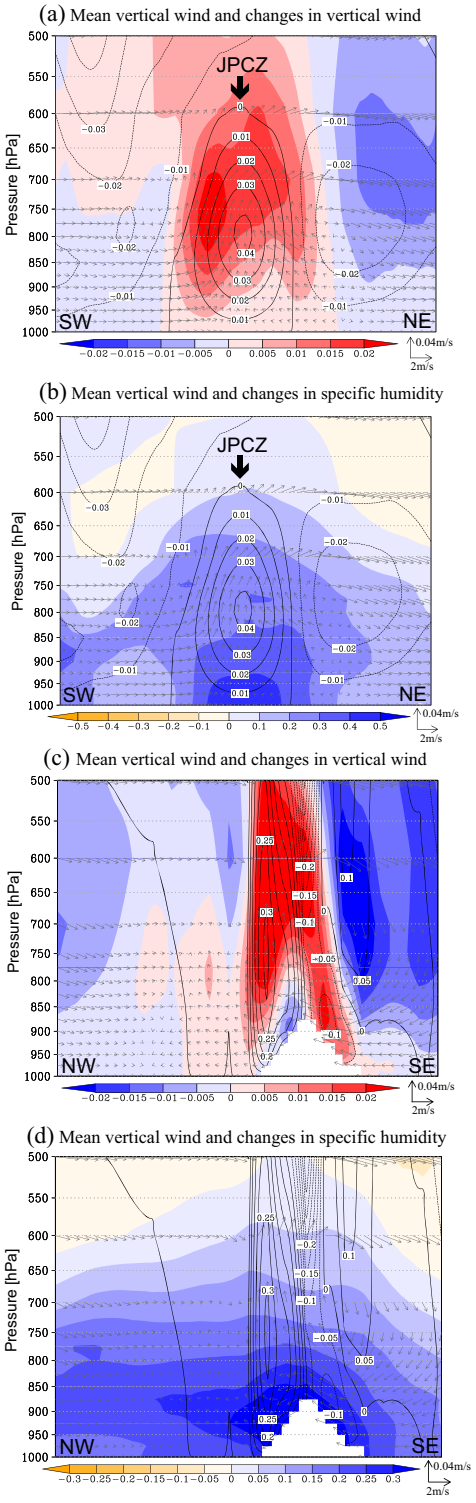

Fig. 5 Vertical cross sections of wind and specific humidity of the top 50 heavy snowfall events at GP_INLAND. The vertical wind speed in the historical simulations is indicated as contours, and the difference between the historical and future climate simulations in the vertical and horizontal winds are indicated as vectors. *Shaded areas* indicate the differences in (**a**, **c**) vertical wind speed and (**b**, **d**) specific humidity. *Warm colors* represent an upward wind anomaly in the future climate. SW, NE, SE, and NW correspond to the directions in Fig. 4b

Although precipitation is intensified (Fig. 4b), snowfall decreases remarkably over the Sea of Japan and in the coastal area of central Japan (Fig. 4c) since the conversion of snowfall to rainfall is dominant due to warming. Snowfall is intensified in the inland area of central Japan where the surface air temperature is still below 0 °C in the future climate. Since JP_middle is not influenced by the JPCZ, and the mountains in this area are lower than those in JP_central, the enhancement of heavy snowfall would be unclear (Figs. 1b and 3b).

5 Discussion

Our results indicate that heavy daily snowfall could be intensified by warmed oceans and mesoscale convergence, i.e., the JPCZ and orographic effects. A similar condition is found on the leeward side of the Great Lakes (Hjelmfelt 1990; Burnett et al. 2003) and Great Salt Lake (Steenburgh et al. 2000) in North America, which is called the lake effect. Land breezes from both shores sometimes converge and cause snowstorms on the leeward side of the Great Lakes and the Great Salt Lake, depending on synoptic conditions (Peace and Sykes 1966; Hjelmfelt 1990; Steiger et al. 2013). Notaro et al. (2015) projected future increases in lake evaporation and total lake-effect precipitation in the mid and late twenty-first century due to reduced ice cover and greater dynamically induced wind fetch, although rainfall increased more at the expense of snowfall. Gula and Peltier (2012) also found that future changes in lake surface temperatures and ice cover may locally increase snowfall as a result of increased evaporation and the enhanced lake effect in the middle of the twenty-first century. Thus, our results suggest that extremely heavy snowfall could also intensify around the Great Lakes due to global warming.

The 20-km NHRCM, however, has precipitation biases that could be caused by its spatial resolution not enough to represent the mountainous regions. The estimated heights of mountains in NHRCM with 20-km grid spacing are lower than their actual heights, leading to less vertical motions and less orographic enhancement of precipitation (Ishizaki et al. 2012; Kawase et al. 2015b). To accurately simulate smaller-scale convective snowfall developing over the Sea of Japan, cloud-resolving simulations without the cumulus convective parameterization are needed, which can affect the snowfall in the coastal areas. In addition, extremely heavy daily snowfall may be influenced by the interaction of the atmosphere and ocean over the Sea of Japan. Ensemble simulations by CGCMs or AGCMs with a slab ocean model would be needed in the future.

6 Summary

By analyzing the outputs of the large ensemble regional climate simulations of the d4PDF, we investigated future changes in extremely heavy snowfall in Japan under global warming conditions when the global mean surface air temperature is 4 °C higher than the pre-industrial climate. In the future climate simulations, extremely heavy daily snowfall events occur more frequently in the inland areas on the Sea of Japan coast than in the historical climate simulations. The enhancement of heavy snowfall is also projected in the northern part of Japan and the northeastern part of the Asian continent where the winter mean temperature is much lower than the freezing point of water, and the total snowfall amount increases. A

composite analysis of extremely heavy snowfall events in central Japan indicates that extremely heavy precipitation occurs when the JPCZ is present over the Sea of Japan during the EAWM season. In the future climate projections, the JPCZ could be intensified since the warm ocean supplies much water vapor. By simple thermodynamics, moistening due to global warming could enhance precipitation over the upward flow regions, such as the JPCZ and windward side of mountains, if the upward flow were unchanged in the future climate. An upward wind anomaly is also found over the windward side of mountains where the upward flow is prevalent climatologically. Both the strengthened JPCZ and the enhancement of upward wind over mountain ranges could result in heavy snowfall in the mountainous areas in central Japan. In the future, it will be necessary to monitor extremely heavy snowfall in the inland area of central Japan, where the surface air temperature will still be lower than 0 °C in winter.

Acknowledgments We thank all members of MRI, AORI, NIES, DPRI, JAMSTEC, and the University of Tsukuba, who built up d4PDF. The Earth Simulator was used in this study as a "Strategic Project with Special Support" of JAMSTEC. Also, the study was supported by the Program for Risk Information on Climate Change (SOUSEI) and the Data Integration and Analysis System (DIAS), both of which are sponsored by the Ministry of Education, Culture, Sports, Science and Technology of Japan. This study was partly supported by JSPS KAKENHI Grant Number 26750111. The dataset of d4PDF is available from the website of DIAS (http://www.editoria.u-tokyo.ac.jp/projects/dias.old2/?locale=en).

References

Armstrong RL, Brun E (eds) (2008) Snow and climate: physical processes, surface energy exchange and modeling. Cambridge University Press, Cambridge, 222 pp

Brown RD, Mote P (2009) The response of Northern Hemisphere snow cover to a changing climate. J Clim 22: 2124–2145

Burnett AW, Kirby ME, Mullins HT, Patterson WP (2003) Increasing Great Lake-effect snowfall during the twentieth century: a regional response to global warming? J Clim 16:3535–3542

Collins M, Knutti R, Arblaster J, et al. (2013) Long-term climate change: projections, commitments and irreversibility. In: Stocker TF et al. (eds) Climate Change 2013: The Physical Science Basis, Contribution of Working Group I to the Fifth Assessment Report of the Intergovernmental Panel on Climate Change, chap. 12. Cambridge Univ. Press, Cambridge

de Vries H, Lenderink G, van Meijgaard E (2014) Future snowfall in western and central Europe projected with a high-resolution regional climate model ensemble. Geophys Res Lett 41:4294–4299. doi:10.1002/2014GL059724

Gula J, Peltier RW (2012) Dynamical downscaling over the Great Lakes basin of North America using the WRF regional climate model: the impact of the Great Lakes system on regional greenhouse warming. J Clim 25: 7723–7742

Heo KY, Ha KJ (2008) Snowstorm over the southwestern coast of the Korean Peninsula associated with the development of mesocyclone over the Yellow Sea. Adv Atmos Sci 25(5):765–777. doi:10.1007/s00376-008-0765-2

Hirahara S, Ishii M, Fukuda Y (2014) Centennial-Scale Sea surface temperature analysis and its uncertainty. J Clim 27:57–75. doi:10.1175/JCLI-D-12-00837.1

Hjelmfelt MR (1990) Numerical study of the influence of environmental conditions on lake-effect snowstorms over Lake Michigan. Mon Weather Rev 118:138–150

Ishizaki NN, Takayabu I, Oh'izumi M, et al. (2012) Improved performance of simulated Japanese climate with a multi-model ensemble. J Meteorol Soc Jpn 90:235–254

Kawase H, Hara M, Yoshikane T, et al. (2013) Altitude dependence of future snow cover changes over Central Japan evaluated by a regional climate model. J Geophys Res 118:12444–12457. doi:10.1002/2013JD020429

Kawase H, Suzuki C, Ishizaki NN, et al. (2015a) Simulations of monthly variation in snowfall over complicated mountainous areas around Japan's Northern Alps. SOLA 11:138–143. doi:10.2151/sola.2015-032

Kawase H, Sasaki H, Murata A, et al. (2015b) Future changes in winter precipitation around Japan projected by ensemble experiments using NHRCM. J Meteorol Soc Jpn 93:571–580. doi:10.2151/jmsj.2015-034

Lim K-S, Hong S-Y (2007) Numerical simulation of heavy snowfall over the Ho-Nam province of Korea in December 2005. J Korean Meteorol Soc 43:161–173

Lute AC, Abatzoglou JT, Hegewisch KC (2015) Projected changes in snowfall extremes and interannual variability of snowfall in the western United States. Water Resour Res 51:960.972. doi:10.1002/2014WR016267

Ma X, Yoshikane T, Hara M, et al. (2010) Hydrological response to future climate change in the Agano River basin, Japan. Hydrol Res Lett 4:25–29

Manabe S (1957) On the modification of air-mass over the Japan Sea when the outburst of cold air predominates. J Meteorol Soc Jpn 35:311–326

Mizuta R, Yoshimura H, Murakami H, et al. (2012) Climate simulations using MRI-AGCM with 20-km grid. J Meteorol Soc Jpn 90(A):233–258

Mizuta R, Arakawa O, Ose T, et al. (2014) Classification of CMIP5 future climate responses by the tropical sea surface temperature changes. SOLA 10:167–171. doi:10.2151/sola.2014-035

Nagata M, Ikawa M, Yoshizumi S, Yoshida T (1986) On the formation of a convergent cloud band over the Japan Sea in winter; numerical experiments. J Meteorol Soc Jpn 64:841–855

Notaro M, Bennington V, Vavrus S (2015) Dynamically downscaled projections of lake-effect snow in the Great Lakes basin. J Clim 28:1661–1684. doi:10.1175/JCLI-D-14-00467.1

O'Gorman PA (2014) Contrasting responses of mean and extreme snowfall to climate change. Nature 512(7515):416–418

Peace RL, Sykes RB Jr. (1966) Mesoscale study of a lake-effect snowstorm. Mon Weather Rev 94(8):495–507

Räisänen J, Eklund J (2012) Twenty-first century changes in snow climate in northern Europe: A high-resolution view from ENSEMBLES regional climate models. Clim Dyn 38:2575–2591. doi:10.1007/s00382-011-1076-3

Rasmussen R, Liu C, Ikeda K, et al. (2011) High-resolution coupled climate runoff simulations of seasonal snowfall over Colorado: a process study of current and warmer climate. J Clim 24:3015–3048

Sasaki H, Kurihara K, Takayabu I, Uchiyama T (2008) Preliminary experiments of reproducing the present climate using the non-hydrostatic regional climate model. SOLA 4:25–28. doi:10.2151/sola.2008-007

Shi X, Durran DR (2015) Estimating the response of extreme precipitation over midlatitude mountains to global warming. J Clim 28(10):4246–4262

Siler N, Roe G (2014) How will orographic precipitation respond to surface warming? An idealized thermodynamic perspective. Geophys Res Lett 41. doi:10.1002/2013GL059095

Steenburgh WJ, Halvorson SF, Onton DJ (2000) Climatology of lake-effect snowstorms of the Great Salt Lake. Mon Weather Rev 128:709–727

Steger C, Kotlarski S, Jonas T, Schär C (2012) Alpine snow cover in a changing climate: a regional climate model perspective. Clim Dyn 41:735–754. doi:10.1007/s00382-012-1545-3

Steiger SM, Schrom R, Stamm A, et al. (2013) Circulations, bounded weak echo regions, and horizontal vortices observed within long-lake-axis-parallel-lake-effect storms by the Doppler on wheels. Mon Weather Rev 141(8):2821–2840

Sun J, Wang H, Yuan W, Chen H (2010) Spatial-temporal features of intense snowfall events in China and their possible change. J Geophys Res 115:D16110. doi:10.1029/2009JD013541

Vaughan DG, Comiso JC, Allison I, et al. (2013) Observations: cryosphere. In: Stocker TF et al. (eds) Climate Change 2013: The Physical Science Basis, Contribution of Working Group I to the Fifth Assessment Report of the Intergovernmental Panel on Climate Change, chap. 4. Cambridge Univ. Press, Cambridge

Wi S, Dominguez F, Durcik M, Valdes J, et al. (2012) Climate change projection of snowfall in the Colorado River Basin using dynamical downscaling. Water Resour Res 48:W05504. doi:10.1029/2011WR010674